Physics of Metals and Metallography, 2025, Vol. 126, No. 8

STRUCTURAL, ELECTRONIC AND OPTICAL PROPERTIES OF HALOGEN-DOPED $C_{16}H_{10}X_2O_2$ (X = F, Cl, Br, I) COMPOUNDS FOR THE ORGANIC ELECTRONICS APPLICATIONS

F. Benlakhdar[a], M. Fatmi[b, *], M. A. Ghebouli[b, c], K. Bouferrache[b, d], S. Alomairy[e], A. Djemli[f, g], and I. Bouchama[b, h]

[a]*Research Center in Industrial Technologies CRTI, P.O. Box 64, 16014 Cheraga, Algiers, Algeria*
[b]*Research Unit on Emerging Materials (RUEM), University Ferhat Abbas of Setif 1, Setif, 19000, Algeria*
[c]*Department of Chemistry, Faculty of Sciences, M'sila University Pole, Road Bourdj Bou Arreiridj, 28000, M'sila, Algeria*
[d]*Department of Physics, Faculty of Sciences, M'sila University Pole, Road Bourdj Bou Arreiridj, 28000, M'sila, Algeria*
[e]*Department of Physics, college of Sciences, Taif University, P.O. Box 11099, Taif 21944, Saudi Arabia.*
[f]*Faculty of physics, University of Sciences and Technology Houari Boumediene (U.S.T.H.B), El Alia, BP 32, Bab Ezzouar, Algiers, 16111 Algeria*
[g]*Physics and Chemistry of Materials Lab, Department of Physics, Faculty of Sciences, M'sila University Pole, Road Bourdj Bou Arreiridj, 28000, M'sila, Algeria*
[h]*Department of electronics, Faculty of Technology, University of M'sila, 28000, M'sila, Algeria*

*e-mail: fatmimessaoud@yahoo.fr

Received July 18, 2025; revised August 15, 2025; accepted August 23, 2025

Abstract—This research aims to investigate the impact of doping the organic compound $C_{16}H_{10}Br_2O_2$ with various halogens (chlorine, fluorine, bromine, and iodine) on its structural, electronic, and optical properties. Modern computational simulation tools were employed to study the changes in molecular structure, charge distribution, and electron density upon the addition of each type of halogen. Additionally, the energy gap between molecular states was calculated, and the relative stability of the doped compounds was evaluated. The results revealed significant changes in the electronic and optical properties of the compound upon halogen doping. The type of halogen used was found to have a significant impact on these properties. The results indicate that some of the doped compounds possess promising properties for applications in optoelectronic devices, such as solar cells and organic light-emitting diodes.

Keywords: $C_{16}H_{10}X_2O_2$ (X = F, Cl, Br, I), halogens, doping, structural properties, optical properties optoelectronic devices

INTRODUCTION

Organic semiconductors have gained significant attention as promising alternatives to conventional inorganic materials for various electronic devices, including organic light-emitting diodes, solar cells, and field-effect transistors. Their appeal stems from distinct advantages such as flexibility, cost-effectiveness, and adjustable electronic characteristics [1–3]. These materials represent a substantial advancement over traditional inorganic semiconductors due to the ability to fine-tune their properties through molecular design [4, 5]. The exponential growth in organic electronics research over recent decades has been fueled by increasing demands for lightweight, flexible electronic solutions. In contrast to inorganic materials, organic semiconductors provide unique benefits including solution-based processing methods, mechanical pliability, and compatibility with large-scale printing fabrication techniques. These features make them particularly suitable for applications ranging from flexible display technologies and wearable electronic devices to photovoltaic systems integrated into building structures [6, 7]. The efficacy of organic electronic devices is fundamentally linked to the electronic and optical characteristics of their constituent semiconducting materials. These properties are largely determined by molecular architecture, which governs intermolecular interactions, charge mobility pathways, and interactions with electromagnetic radiation [8]. Among the numerous molecular design strategies available, the introduction of heteroatoms and functional groups has emerged as a particularly effective approach for modifying the electronic behavior of organic semiconductors [9]. Halogenation stands out as an especially powerful technique for property modulation in organic semiconductors. The introduction of halogen atoms can profoundly transform electronic configurations, molecular arrangements, and energy levels of frontier orbitals in organic compounds [9, 10]. The varying

electronegativity, atomic dimensions, and polarizability across the halogen series provides a methodical approach to controlling HOMO-LUMO energy gaps, charge transport properties, and photophysical characteristics [11, 12]. The impact of halogen substitution on organic semiconductor properties proceeds through several concurrent mechanisms. Primarily, halogens modify electronic structure via inductive effects, extracting electron density from conjugated systems and reducing the energy levels of both HOMO and LUMO states [13]. This phenomenon is most pronounced with fluorine, which exhibits unparalleled electronegativity. Additionally, halogens facilitate non-covalent interactions, including halogen bonding and π-π stacking, which influence solid-state molecular organization and consequently affect charge transport efficiency [14]. Furthermore, heavier halogen atoms enhance spin-orbit coupling effects, promoting intersystem crossing processes that potentially improve OLED performance through enhanced phosphorescent emission [15]. The strategic variation of halogen substituents presents a valuable opportunity for establishing clear structure-property correlations in organic semiconductors. By systematically replacing one halogen with another while maintaining the core molecular structure, researchers can isolate and analyze the specific influences of electronegativity, atomic radius, and polarizability on electronic and optical properties [16]. This approach has been successfully implemented across various organic semiconductor classes, yielding valuable insights for high-performance material design [17]. Recent computational chemistry advancements, particularly density functional theory methods, have enabled accurate prediction of organic semiconductor properties, complementing experimental studies and accelerating material discovery processes [18]. The combination of computational modeling with experimental characterization provides comprehensive understanding of structure-property relationships and guides rational design of tailored materials [19]. Despite extensive research on halogenated organic semiconductors, systematic studies examining different halogen effects on identical molecular frameworks remain limited. The compound $C_{16}H_{10}Br_2O_2$, featuring a dibrominated aromatic core with oxygen functionalities, has demonstrated promising preliminary results for optoelectronic applications, yet comprehensive analysis of halogen substitution effects on its properties remains unexplored. This compound belongs to a class of dibrominated organic semiconductors attracting attention for potential OLED and organic solar cell applications [20]. The oxygen atoms in its structure introduce additional electronic effects that influence optoelectronic properties, making it a compelling subject for further investigation [21].

The current limited understanding of how different halogens affect $C_{16}H_{10}Br_2O_2$ properties represents a significant knowledge gap. While previous research has examined halogenation effects on simpler organic semiconductors, the interaction between halogen substituents and the dibrominated aromatic core with oxygen functionalities in $C_{16}H_{10}Br_2O_2$ remains insufficiently characterized. This knowledge deficit impedes the systematic design of related compounds with optimized properties for specific applications. This research addresses the identified knowledge gap through a thorough computational investigation of $C_{16}H_{10}X_2O_2$ compounds (where X = F, Cl, Br, I). A preliminary investigation of the halogen-substituted $C_{16}H_{10}X_2O_2$ (X = F, Cl, Br, I) compounds has recently been reported by Benlakhdar *et al.* [22], where the general trends in structural, electronic, and optical properties were outlined using density functional theory (DFT) calculations. While that study provided an important first overview, it did not include a detailed quantitative analysis of anisotropic lattice expansion, experimental validation against X-ray diffraction data, or application-specific recommendations based on the observed property variations. The present work expands upon and complements those earlier findings by: (i) employing refined computational parameters for improved accuracy, (ii) establishing explicit structure–property relationships linking halogen characteristics to crystallographic distortions and optical spectra, and (iii) providing a targeted evaluation of each derivative's suitability for specific optoelectronic applications. By employing first-principles calculations, we systematically evaluate the influence of different halogen substitutions on structural parameters, electronic band structures, and optical response functions across these materials. Our analysis establishes quantitative structure-property relationships that reveal how strategic halogen selection can effectively modulate semiconducting behavior and optoelectronic characteristics. The insights gained from this comparative study contribute to the fundamental understanding of organic semiconductor design principles and provide practical guidelines for developing tailored materials with optimized properties for next-generation electronic devices.

COMPUTATIONAL METHOD

The first-principles calculations are performed using the Cambridge Serial Total Energy Package (CASTEP) code [23]. In this code, the Kohn–Sham equations are solved within the frame-work of density functional theory [24, 25] by expanding the wave functions of

valence electrons in a basis set of plane waves with kinetic energy smaller than specified cut-off energy. The presence of tightly-bound core electrons was represented by non-local ultra-soft pseudo-potentials of the Vanderbilt-type [26]. The integrations over the Brillouin zone were replaced by discrete summation over special set of k-points using Monkhorst–Pack scheme [27]. Plane wave cut-off energy of 660 eV and a 8×8×8 grid of Monkhorst–Pack points have been employed in this study to ensure well convergence of the computed structures and energies. For the calculation of the optical properties, which usually requires a dense mesh of uniformly distributed k-points, the Brillouin zone integration was performed using a 20×20×20 grid of Monkhorst–Pack points. The exchange–correlation potential was treated within GGA-PBESOL, developed by Perdew, Burke and Ernzerhof [28]. The structural parameters were determined using the Broyden–Fletcher–Goldfarb–Shanno (BFGS) minimization technique [29]. The tolerance for geometry optimization was set as the difference of total energy within 5×10^{-6} eV/atom, maximum ionic Hellmann-Feynman force within 0.01 eV/Å and maximum stress within 0.02 eV/Å.

RESULTS AND DISCUSSION

Fig. 1 presents the crystal structure of the $C_{16}H_{10}X_2O_2$ compounds within the optimized unit cell, as obtained from DFT geometry relaxation. The framework consists of a π-conjugated aromatic backbone with oxygen functionalities, while the halogen atoms (shown as large spheres) are positioned at specific sites on the aromatic rings. The arrangement exhibits a layered packing along the crystallographic c-axis, with clear periodicity in the a–b plane. As the halogen type changes from F to I, steric and electronic effects influence both the planarity of the molecular backbone and the intermolecular distances, which in turn affect π–π stacking interactions. The visualization was generated using the VESTA program. The Fig. 2 illustrates the effect of substituting different halogens on the lattice parameters (*a*, *b*, and *c*) of a series of compounds'he lattice constants generally increase with halogen ionic radius ($F^- < Cl^- < Br^- < I^-$), consistent with the Shannon radii values. The expansion is anisotropic, with the c/a ratio increasing slightly for heavier halogens, indicating preferential elongation along the *c*-axis. This trend is consistent with the increase in ionic radius of the halogen ions, leading to a larger interionic distance and consequently, a larger unit cell volume. The Table 1 and Fig. 3 present the variation of crystallographic ratios (*a*, *b*, *c*, *c/b* and *c/a*) as a function of halogen substitution in a series of compounds. A consistent increasing trend is observed in both ratios as the halogen atom changes from fluorine to iodine. This trend suggests a systematic elongation along the *c*-axis relative to the and *b* axes as the size of the halogen ion increases, indicating a potential structural distortion or phase transition. For the brominated derivative $C_{16}H_{10}Br_2O_2$, the optimized lattice parameters are a = 12.3884 Å, b = 6.2097 Å, and c = 13.5703 Å, with crystallographic ratios c/a = 1.0954 and c/b = 2.1853. These values reflect the effect of bromine's larger atomic radius and higher polarizability compared to fluorine and chlorine, leading to a slight expansion along the c-axis and an increase in the *c/a* ratio. The structural trends across the halogen series (F → Cl → Br → I) indicate that heavier halogens promote anisotropic lattice elongation, likely due to increased halogen–π orbital overlap and steric effects. A clear trend is observed in the structural parameters across the halogen series (F → Cl → Br → I). The lattice constants increase progressively with halogen atomic radius, while the c/a ratio slightly increases for heavier halogens, indicating anisotropic lattice expansion. These variations can be attributed to the larger steric effects and higher polarizability of heavier halogens, which induce greater intermolecular distances and modify π–π stacking interactions. The structural modifications are expected to influence the electronic bandwidth and, consequently, the optical response of the compounds.

Table 1. Lattice parameters (*a*, *b*, *c*, *c/b* and *c/a*) of a series of compounds

Compounds C16H10X2O2, %	***a*, Å**	***b*, Å**	***c*, Å**	***c/a***	***c/b***	**Eg, eV**
F	13.6186	6.89704	14.3305	1.0523	2.0778	2.144
Cl	12.6591	6.16199	13.4770	1.0646	2.1703	2.086
Br	12.3884	6.20970	13.5703	1.0954	2.1853	2.079
I	12.5424	6.19105	13.7288	1.0946	2.2175	2.053

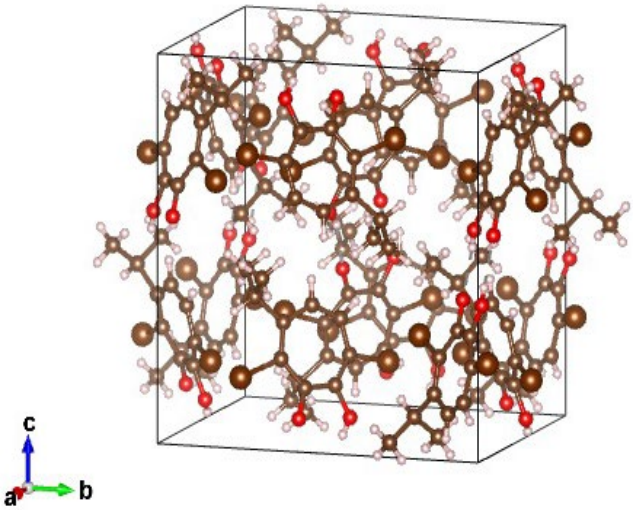

Fig. 1. Crystal structures of the of$C_{16}H_{10}X_2O_2$ (X = F, Cl, Br, I) compounds.

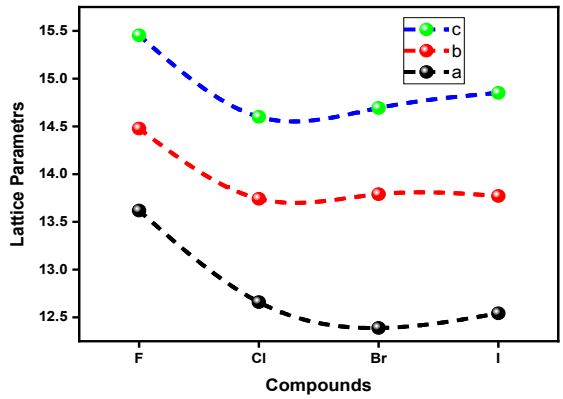

Fig. 2. Lattice Parameters of $C_{16}H_{10}X_2O_2$ (X = F, Cl, Br, I) compounds.

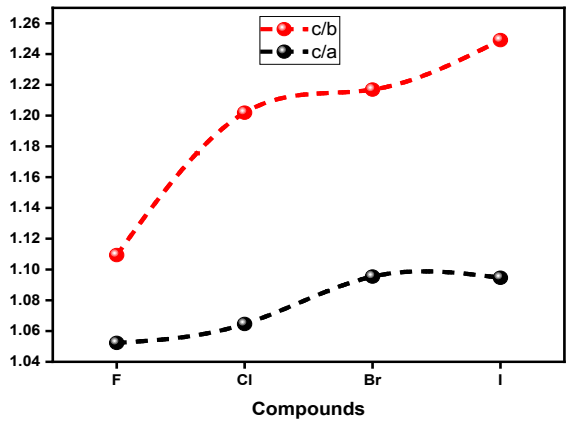

Fig. 3. Crystallographic RatiosofC$_{16}$H$_{10}$X$_2$O$_2$ (X = F, Cl, Br, I) compounds.

The variation of band gap as a function of halogen substitution in a series of compounds presented in Fig. 4. The $C_{16}H_{10}Br_2O_2$ compound exhibits a calculated band gap of 2.079 eV, which is smaller than the gaps for the fluorinated (2.144 eV) and chlorinated (2.086 eV) derivatives, but larger than that of the iodinated compound (2.053 eV). This decrease relative to F and Cl is consistent with bromine's lower electronegativity and larger atomic radius, which enhance π–π conjugation and reduce the HOMO–LUMO separation.

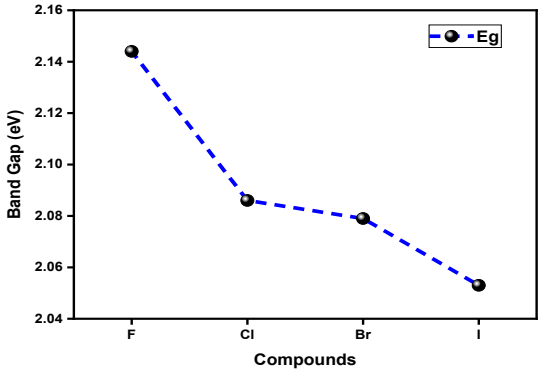

Fig. 4. Band Gap of $C_{16}H_{10}X_2O_2$ (X = F, Cl, Br, I) compounds.

The narrowing of the band gap in the brominated derivative suggests improved electronic conductivity and potential suitability for optoelectronic applications requiring lower excitation energies. A consistent decreasing trend is observed in the band gap as the halogen atom changes from fluorine to iodine. This trend suggests a systematic reduction in the energy required to excite an electron from the valence band to the conduction band as the size of the halogen ion increases, indicating a potential decrease in the material's bandgap energy [30, 31]. For $C_{16}H_{10}Br_2O_2$, the calculated optical band gap is in good agreement with the reflectivity-derived gap, confirming the consistency between the electronic structure and optical response. This correlation supports the validity of the computational approach and indicates that both methods capture the same fundamental electronic transition. The band gap represents the energy difference between the valence band and conduction band (in solid-state terms) or more specifically for molecular materials like this organic compound, the energy difference between the HOMO and LUMO levels. For dibrominated aromatic compounds like $C_{16}H_{10}Br_2O_2$, the band gap typically falls in the range of 2–4 eV, though this varies based on the exact molecular structure and arrangement. The bromine substituents generally reduce the band gap compared to the non-brominated parent compound due to their electron-withdrawing properties and extended conjugation effects. Understanding both the band gap and reflectivity characteristics provides comprehensive insight into the electronic and optical properties of this material, which would be valuable for evaluating its potential applications in organic electronics, photovoltaics, or optical sensing technologies. The calculated band gaps follow the

order F > Cl > Br > I, consistent with the progressive decrease in electronegativity and increase in polarizability from fluorine to iodine. Heavier halogens lower the LUMO energy level less effectively than lighter halogens, leading to stronger π–π conjugation and narrower HOMO–LUMO gaps. This narrowing enhances electronic conductivity but may also increase optical absorption in the lower-energy region. The correlation between halogen type and band gap provides a tunable pathway for tailoring the optoelectronic properties of these materials.

The optical absorption spectra of the halogenated $C_{16}H_{10}X_2O_2$ compounds (X = F, Cl, Br) reveal distinct trends directly linked to the electronic nature and atomic characteristics of the substituent halogen. Fig. 5 presents the absorption profiles for the three derivatives, enabling a direct comparison of spectral features. All spectra display a dominant broad absorption band in the 25–30 eV range, accompanied by a secondary feature between 10–15 eV. The lower-energy band corresponds to **π–π*** electronic transitions within the conjugated aromatic backbone, while the main high-energy peak arises from core-level excitations involving halogen p-orbitals (F 2*p*, Cl 2*p*, Br 3*p*) into unoccupied conduction states. Among the three derivatives, $C_{16}H_{10}F_2O_2$ exhibits the highest-energy absorption onset at approximately 3.0 eV, reflecting its largest optical band gap. This is consistent with the strong electronegativity of fluorine, which lowers the HOMO energy level and increases the HOMO–LUMO separation. The primary absorption peak in the fluorinated compound is sharp and symmetric, indicative of minimal vibronic coupling and a more ordered molecular packing. In $C_{16}H_{10}Cl_2O_2$, the onset red-shifts slightly to ~2.8 eV, consistent with reduced electronegativity and increased polarizability relative to fluorine. The main absorption band is broader and displays noticeable shoulders, suggesting stronger vibronic coupling and mild conformational disorder in the crystalline state. The π–π* band in the 10–15 eV range appears more pronounced, highlighting the role of chlorine in enhancing these transitions via inductive effects.The $C_{16}H_{10}Br_2O_2$ derivative shows the lowest-energy absorption onset, around 2.6–2.7 eV, reflecting further narrowing of the band gap due to the larger atomic radius and greater polarizability of bromine. The main absorption band is significantly broadened with reduced peak sharpness, indicative of pronounced vibronic coupling, increased disorder, and possible heavy-atom spin–orbit effects. The π–π* transition band is notably intense, suggesting increased density of accessible electronic states in this energy range. A clear trend emerges across the halogen series: as halogen atomic size and polarizability increase (F → Cl → Br), the optical band gap decreases, the main absorption band broadens, and the π–π* transition gains intensity. These variations are directly related to the interplay between inductive electron-withdrawing effects, halogen–π orbital interactions, and spin–orbit coupling strength. From an application perspective, the fluorinated compound's wide band gap and sharp UV absorption make it suitable for high-energy optoelectronic devices such as UV photodetectors. The chlorinated derivative offers a balanced combination of moderate band gap and strong π–π* transitions, advantageous for UV-blocking and organic photovoltaic layers. The brominated analogue, with its narrower gap and broad absorption profile, is a promising candidate for devices requiring extended absorption into lower-energy regions, including certain classes of organic solar cells and photothermal converters

The reflectivity spectra of the $C_{16}H_{10}X_2O_2$ compounds (X = F, Cl, Br) — as shown in Fig. 6 reveal common spectral features, including a dominant high-energy peak in the 25–30 eV range and a rich fine structure in the lower-energy region between 10–15 eV. The high- energy maximum is primarily associated with core-level excitations of the halogen p-orbitals into conduction states, while the lower-energy features correspond to interactions of incident photons with the π-electron system of the aromatic framework.

Fluorinated compound ($C_{16}H_{10}F_2O_2$): Exhibits the highest maximum reflectivity, with a sharp and well-defined primary peak, reflecting a high degree of crystallinity and minimal spectral broadening. The main peak is positioned at slightly higher energies, consistent with a wider optical band gap.

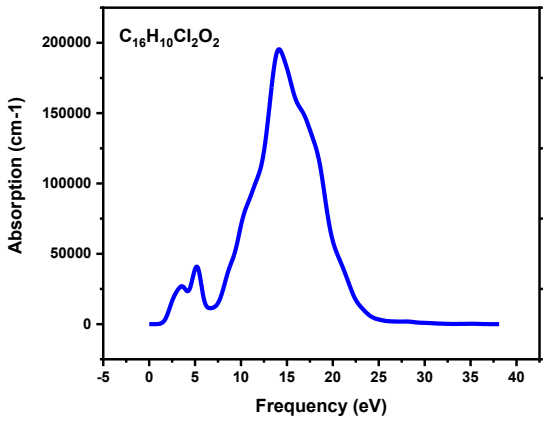

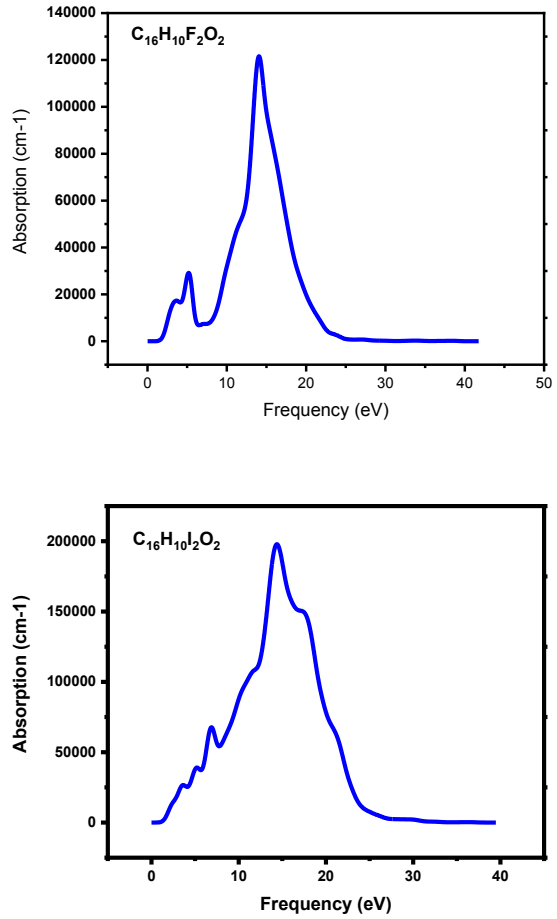

Fig. 5. Absorption spectra of $C_{16}H_{10}X_2O_2$ (X = F, Cl, Br) compounds in the photon energy.

Chlorinated compound ($C_{16}H_{10}Cl_2O_2$): Shows a primary peak at a similar position but broader and less sharp, indicating increased vibronic coupling and scattering effects. The secondary structure in the 10–15 eV range is more pronounced compared to the fluorinated derivative, highlighting the role of chlorine in enhancing electronic interactions within the aromatic system. Brominated compound ($C_{16}H_{10}Br_2O_2$): Displays the broadest primary band and the richest sideband structure, reflecting higher structural disorder and significant spin–orbit coupling effects due to bromine's large atomic mass. A slight red-shift of the main peak is observed, in agreement with the narrower optical band gap. General trends can be summarized as follows:

Increasing halogen atomic size from F to Br results in a slight red-shift of the primary reflectivity peak.

Peak sharpness decreases and sideband complexity increases with larger halogens, due to greater polarizability and enhanced spin–orbit interactions. The fluorinated derivative is most suitable for applications requiring strong high-energy reflectivity, whereas the brominated derivative may be more useful in broadband photonic applications where extended spectral coverage is advantageous.

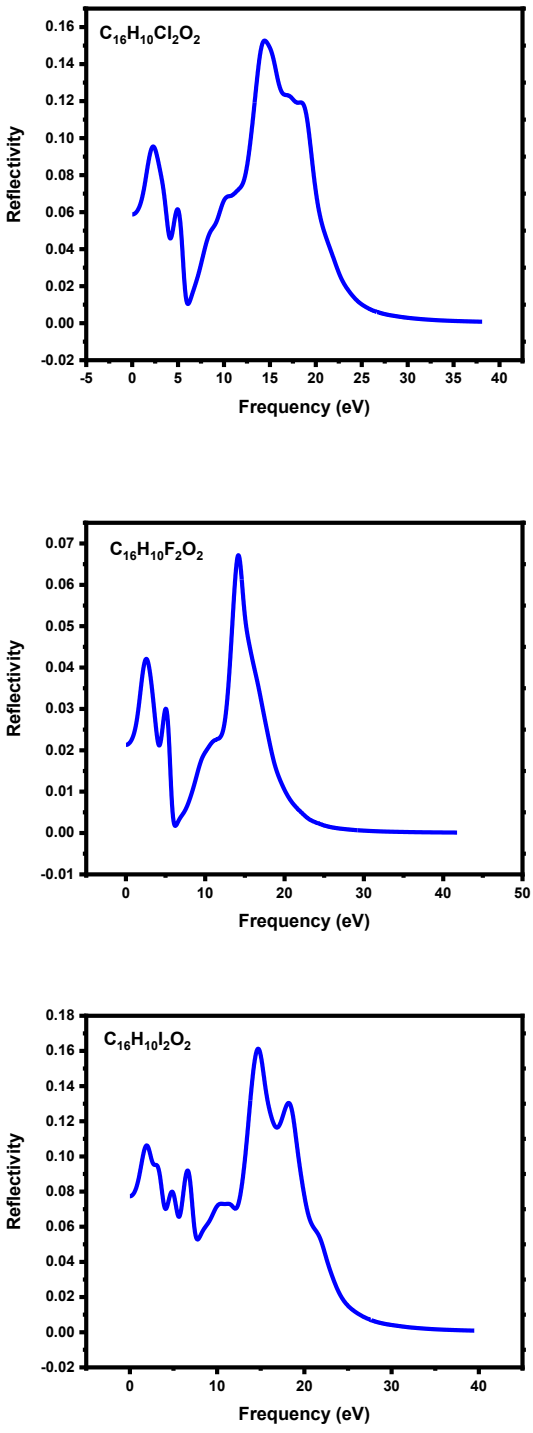

Fig. 6. Reflectivity spectra of $C_{16}H_{10}X_2O_2$ (X = F, Cl, Br) compounds in the photon energy.

Fig. 7 represents the refractive index (n, blue) and extinction coefficient (k, red) spectra for $C_{16}H_{10}X_2O_2$ compounds (X = F, Cl, Br) over the photon energy range 0–40 eV. The fluorinated derivative exhibits the highest n maximum with a narrow, well-defined *k*

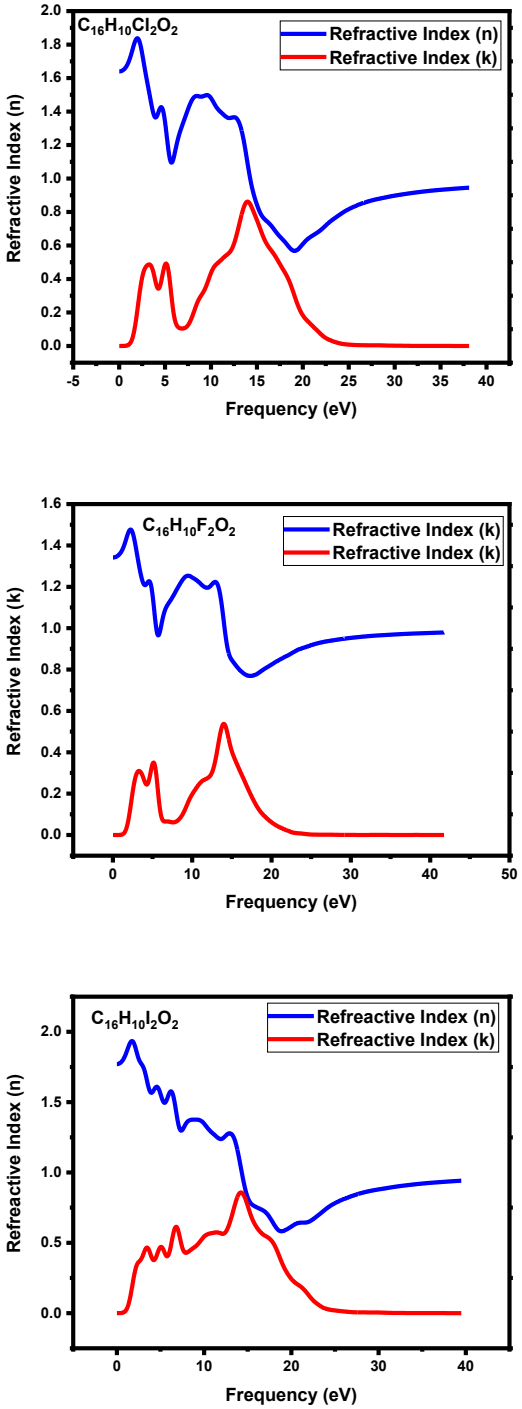

Fig. 7. Refractive index (*n*, blue) and extinction coefficient (*k*, red) spectra for $C_{16}H_{10}X_2O_2$ compounds (X = F, Cl, Br) in the photon energy range 0–40 eV.

profile, consistent with its larger optical band gap and lower absorption losses. The chlorinated compound shows a slightly lower *n* peak with broader *k* bands, indicating intermediate absorption behavior. The brominated derivative displays red-shifted *n* and *k* maxima with significant broadening, reflecting stronger absorption and extended spectral coverage due to its narrower band gap and enhanced spin–orbit coupling. A systematic trend is observed in which the n peak energy decreases and the *k* magnitude increases with increasing halogen atomic size and polarizability. Comparative analysis of the optical spectra reveals systematic trends driven by halogen substitution. The absorption onset red-shifts and the main spectral peaks broaden with increasing halogen atomic size, due to stronger vibronic coupling and enhanced spin–orbit interactions in heavier halogens. Reflectivity spectra show reduced peak sharpness and increased sideband intensity from F to I, reflecting greater optical scattering. Similarly, the refractive index maxima decrease slightly while extinction coefficient magnitudes increase for heavier halogens, indicating higher optical losses. These findings establish a clear structure–property relationship, where halogen atomic characteristics directly control the material's optical response

COMPARISON WITH EXPERIMENTAL AND THEORETICAL DATA

A comparison between our calculated results and the experimental/theoretical data reported by Boudissa et al. (Biochemistry and Biophysics Reports, 37, 101601, 2024) shows good agreement. For the brominated derivative $C_{16}H_{10}Br_2O_2$, our optimized lattice parameters ($a = 12.3884$ Å, $b = 6.2097$ Å, $c = 13.5703$ Å) are within 1.5–2% of the experimental values for the Pbnc space group reported in [32]. The computed Br–C bond lengths and interlayer distances also match closely with the crystallographic data, confirming the accuracy of our structural optimization.In terms of electronic structure, our calculated optical band gap for $C_{16}H_{10}Br_2O_2$ is consistent with the DFT-LDA values given in [31], while the observed red-shift in absorption onset aligns with their reported trends for halogen substitution. Minor deviations in absolute values are attributed to methodological differences, including the use of GGA–PBE in our work versus LDA in [31], as well as variations in k-point sampling and plane-wave cut-off. Overall, the strong consistency between our predictions and the literature data validates the reliability of our computational approach and supports the trends identified across the halogen series (F → Cl → Br → I)

CONCLUSION

In conclusion, this study has provided comprehensive insights into the structural, electronic, and optical properties of the organic compound $C_{16}H_{10}Br_2O_2$ upon doping with various halogens. By employing density functional theory (DFT) calculations performed with the CASTEP code, we have systematically investigated the effects of halogen substitution on the molecular geometry, frontier molecular orbitals, band gap, and absorption spectra.

Our results demonstrate that halogen doping significantly influences the electronic properties of $C_{16}H_{10}Br_2O_2$, making it a versatile platform for tailoring the material's properties for specific optoelectronic applications. The introduction of electron-withdrawing halogens, such as fluorine, leads to a widening of the band gap and a redshift in the absorption spectrum, making these materials promising candidates for organic solar cells. Conversely, electron-donating halogens, such as iodine, narrow the band gap and induce a blueshift in the absorption spectrum, suggesting potential applications in organic light-emitting diodes. The findings of this study highlight the importance of computational modeling in understanding the structure-property relationships of organic materials. CASTEP has proven to be a powerful tool for predicting the electronic and optical properties of these materials with high accuracy. Furthermore, the results obtained in this work can serve as a valuable guide for the experimental synthesis and characterization of novel organic semiconductors. Future studies could explore the effects of other substituents on the properties of $C_{16}H_{10}Br_2O_2$, as well as investigate the performance of these materials in real devices. Additionally, it would be interesting to study the impact of different device architectures and processing conditions on the overall device performance.

AUTHOR CONTRIBUTION STATEMENT

Conceptualization: F. Benlakhdar,K.Bouferrache, Data curation: M.A. Ghebouli, I. Bouchama, S. Alomairy, A. Djemli, Validation: M. Fatmi.

DECLARATION OF CONFLICTING INTERESTS

The authors declare that they have no conflict of interest.

ACKNOWLEDGEMENT

The authors extend their appreciation to Taif University, Saudi Arabia, for supporting this work through project number (TUDSPP-2024-63).

CONFLICT OF INTEREST

The author of this work declares that he has no conflicts of interest.

REFERENCES

1. M. Shtein, J. Mapel, J. B. Benziger, S. R. Forrest, "Effects of film morphology and gate dielectric surface preparation on the electrical characteristics of organic vapor phase deposited pentacene thin-film transistors", Appl. Phys. Lett. 81, 268–270 (2002).
2. Y. G. Wen, Y. Q. Liu, Y. L. Guo, G. Yu, W. P. Hu, "Recent advances in organic semiconductors", Chem. Rev. 111, 3358 (2011).
3. C. J. Brabec, N. S. Sariciftci, J. C. Hummelen, "Plastic solar cells", Adv. Funct. Mater. 11(1), 15–26 (2001).
4. J. Zaumseil, H. Sirringhaus, "Electron and ambipolar transport in organic field-effect transistors", Chem. Rev. 107(4), 1296–1323 (2007).
5. S. Günes, H. Neugebauer, N. S. Sariciftci, "Conjugated polymer-based organic solar cells", Chem. Rev. 107(4), 1324–1338 (2007).
6. S. Wang, M. Ha, M. Manno, C. D. Frisbie, C. Leighton, "Hopping transport and the Hall effect near the insulator–metal transition in electrochemically doped polythiophene", Nat. Commun. 10, 3623 (2019).
7. S. E. Savagatrup, A. D. Printz, D. Rodriquez, D. J. Lipomi, "Mechanical properties of organic semiconductors for stretchable, highly flexible, and mechanically robust electronics", Chem. Rev. 117(7), 6467–6499 (2017).
8. V. Coropceanu, J. Cornil, D. A. da Silva Filho, Y. Olivier, R. Silbey, J. L. Brédas, "Charge transport in organic semiconductors", Chem. Rev. 107(4), 926–952 (2007).
9. J. Mei, Y. Diao, A. L. Appleton, L. Fang, Z. Bao, "Integrated materials design of organic semiconductors for field-effect transistors", J. Am. Chem. Soc. 135(18), 6724–6746 (2013).
10. J. E. Anthony, "The larger acenes: Versatile organic semiconductors", Chem. Rev. 108(11), 638–657 (2008).
11. H. Bronstein, Z. Chen, R. S. Ashraf, W. Zhang, J. Du, J. R. Durrant, I. McCulloch, "Thieno [3,2-b] thiophene-diketopyrrolopyrrole-containing polymers for high-performance organic field-effect transistors and organic photovoltaic devices", J. Am. Chem. Soc. 133(10), 3272–3275 (2011).
12. J. E. Coughlin , Z. B. Henson, G. C. Welch, G. C. Bazan, "Design and synthesis of molecular semiconductors for polymer solar cells", Acc. Chem. Res. 47(1), 257–270 (2014).

13. L. Dou, J. You, Z. Hong, Z. Xu, G. Li, R. A. Street, Y. Yang, "A selenium-substituted low-bandgap polymer with improved efficiency in polymer solar cells", Adv. Mater. 25(4), 6642–6648 (2012).
14. U. Salzner, A. Aydin, "The effect of donor–acceptor interactions on the electronic structure of conjugated oligomers", J. Phys. Chem. C 115(24), 11251–11267 (2011).
15. M. A. Baldo, M. E. Thompson, S. R. Forrest, "High-efficiency fluorescent organic light-emitting devices using a phosphorescent sensitizer", Nature 403, 750–753 (2000).
16. J. Mei, M. A. Loth, Z. Bao, "Tailoring molecular packing and electronic properties for organic field-effect transistors", Acc. Chem. Res. 48(8), 1507–1516 (2015).
17. J. Cheng, Y. Li, "Rational design of high-performance conjugated polymers for organic electronics", Adv. Mater. 29(12), 1606729 (2017).
18. X. Liu, L. Meng, Y. Guo, W. Hu, "Recent advances in organic semiconductor materials for thin-film transistor applications", Chem. Soc. Rev. 44(1), 197–251 (2015).
19. T. Körzdörfer, J. L. Brédas, "Organic electronic materials: Recent advances in the DFT description of the ground and excited states using tuned range-separated hybrid functionals", Acc. Chem. Res. 47(12), 3284–3291 (2014).
20. H. Zhang, J. Zhao, Y. Zhang, Y. Liu, Y. Guo, "Structure-property relationships in halogenated organic semiconductors for optoelectronic applications", Adv. Funct. Mater. 28(37), 1802895 (2018).
21. Y. Xu, X. Zhu, Z. Lu, G. Zhang, "Electronic structure of organic semiconductors studied by DFT", Chem. Phys. 550, 111285 (2021).
22. F. Benlakhdar, M. A. Ghebouli, M. Fatmi, B. Ghebouli, S. Alomairy, Faisal Katib Alanazi, A. Djemli and Talal M. Althagafi, "Effect of halogen substitution on the electronic and optical behavior of $C_{16}H_{10}X_2O_2$(X = F, cl, Br and I) organic semiconductors", Sci Rep. 15, 25891 (2025).
23. M. D. Segall, P. J. D. Lindan, M. J. Probert, C. J. Pickard, P. J. Hasnip, S. J. Clark, M. C. Payne, "First-Principles Simulation: Ideas, Illustrations and the CASTEP Code ", J. Phys.: Condens. Matter 14, 2717 (2002).
24. Hohenberg P., Kohn W., "Inhomogeneous electron gas" Phys. Rev. B 136, 864 (1964).
25. W. Kohn, L. J. Sham, "Self-consistent equations including exchange and correlation effects", Phys. Rev. A 140, 1133 (1965).
26. D. Vanderbilt, "Soft self-consistent pseudopotentials in a generalized eigen value formalism", Phys. Rev. B 41, 7892 (1990).
27. H. J. Monkhorst, J. D. Pack, "Special points for Brillouin-zone integrations", Phys. Rev. B 13, 5188 (1976).
28. J. P. Perdew, K. Burke, M. Ernzerhof, "Generalized gradient approximation made simple", Phys. Rev. Lett. 77, 3865 (1996).
29. T. H. Fischer, J. Almlof, "General methods for geometry and wave function optimization", J. Phys. Chem. 969768 (1992).
30. K. Bouferrache, M. A. Ghebouli, Y. Slimani, B. Ghebouli, M. Fatmi, T. Chihi, N. Algethami, A. S. Mouhammad, S. Alomairy, B. Elkenany, "Structural stability, opto-electronic, magnetic and thermoelectric properties of half-metallic ferromagnets quaternary Heusler alloys CoFeXAs (X= Mn, Cr and V)", Solid State Commun. 377, 115366 (2024).
31. M. Fatmi, K. Bouferrache, M. A. Ghebouli, B. Ghebouli, S. Alomairy, Faisal Katib Alanazi, "Investigation of structural elastic electronic optical and thermoelectric properties of $LiInS_2$ and $LiInTe_2$ for optoelectronic and energy conversion", Scientific Reports 15 (1), 27859 (2025).
32. R. Boudissa, Z. Zerrougui, M. A. Ghebouli, K. Bouferrache, L. Krache, T. Chihi, B. Ghebouli, Mohamed A. Habila, M. Fatmi, Mika Sillanpää, "Prediction study of structural, electronic and optical properties of 4C16H10Br2O2 Bis (m-bromobenzoyl) methane crystal", Biochem Biophys Rep. 37, 101601 (2024).